A Comparative Study on Axial Coordination and Ligand Binding in Ferric Mini Myoglobin and Horse Heart Myoglobin

Giampiero De Sanctis,* Giovanni Petrella,† Chiara Ciaccio,†§ Alessandro Feis,‡ Giulietta Smulevich,‡ and Massimo Coletta†§

*Department of Molecular, Cellular and Animal Biology, University of Camerino, I-62032 Camerino (MC), Italy; †Department of Experimental Medicine and Biochemical Sciences, University of Roma Tor Vergata, I-00133 Rome, Italy; ‡Department of Chemistry, University of Firenze, I-50019 Sesto Fiorentino (FI), Italy; and §Interuniversity Consortium for the Research on the Chemistry of Metals in Biological Systems (CIRCMSB), I-87100 Bari, Italy

ABSTRACT The absorption and resonance Raman spectra and the azide binding kinetics of ferric horse heart myoglobin (Mb) and mini myoglobin (a chemically truncated form of horse heart Mb containing residues 32–139) have been compared. The steady-state spectra show that an additional six-coordinated low-spin form (not present in entire horse heart Mb, which is purely six-coordinated high spin) predominates in mini Mb. The distal histidine is possibly the sixth ligand in this species. The presence of two species corresponds to a kinetic biphasicity for mini Mb that is not observed for horse heart Mb. Azide binds to horse heart Mb much more slowly than to sperm whale Mb. This difference may result from a sterically hindered distal pocket in horse heart Mb. In both cases, the rate constants level off at high azide concentrations, implying the existence of a rate-limiting step (likely referable to the dissociation of the axial sixth ligand). The faster rate constant of mini Mb is similar to that of sperm whale Mb, whereas the slower one is similar to that of entire horse heart Mb.

INTRODUCTION

Ligand binding to ferric hemoproteins has been the subject of several studies (1–8), which have indicated the important role of the distal histidine in controlling the binding of anionic ligands such as azide (N_3^-). In sperm whale myoglobin (SWMb), distal histidine (HisE7) appears to regulate azide binding mostly by affecting the dissociation rate constant (which is increased when HisE7 is replaced by a smaller residue (3,9)) without significantly affecting the apparent association rate constant. Therefore, a stabilizing interaction between HisE7 and the bound azide was suggested. This hypothesis was supported by the observation that the rate-enhancing effect of removal of HisE7 was almost counterbalanced by the replacement of ThrE10 by Arg (3,9). In fact, this residue can play the same stabilizing role as the distal histidine, as also observed in Mb, which lacks the distal HisE7 but contains an arginine in position E10 (1,10).

On the other hand, the apparent association rate constant for azide can be controlled by the presence of a H_2O molecule coordinated to the heme because its absence in Mb greatly affects this parameter (1). The presence of coordinated H_2O implies its displacement when azide is bound, giving rise to a rate-limiting step at high azide concentration (5). Therefore, the exchange rate for the H_2O molecule between the heme pocket and the bulk solvent becomes one of the determinants in controlling the binding rate for anionic ligands. As a consequence, the intrinsic association rate constant of any ligand to the (aquo) ferric forms cannot be determined because a competition between the ligand and the H_2O molecule is always present. In this respect, the structural-functional correlations for this process turn out very important for the characterization of the pathway for the ligand exchange between the bulk solvent and the heme pocket.

Recent studies have shown that complete removal of the A helix, associated with partial removal of the B and H helices, can be performed without altering the O_2 and CO binding properties of Fe(II) horse heart myoglobin (HHMb) (11). This so-called mini Mb, containing the amino acid sequence Leu^{32}–Arg^{139} of HHMb misses several H bonds that are relevant for the tertiary structure (12). Therefore, mini Mb may represent an interesting model to study the role played by the missing helices and H bonds in regulating the reactivity of Mb toward anionic ligands. The aim of this work is to compare the spectroscopic properties and the azide binding kinetics of mini Mb (never obtained before) with those of intact HHMb to better understand the role of different portions of the distal side of the heme pocket in defining the ligand exchange pathway with the bulk solvent.

EXPERIMENTAL PROCEDURES

Horse heart Mb was purchased from Sigma (Sigma Chemical, St. Louis, MO), and mini Mb was prepared as previously published (11).

The spectra of horse heart and mini Mb at pH 7.0 were obtained in 100 mM phosphate buffer. The complex Mb-imidazole was obtained in 100 mM Tris buffer, pH 8.4. The concentration of the protein, determined spectrophotometrically using $\varepsilon = 157\ cm^{-1}\ mM^{-1}$ at 409 nm (13), was 60–90 μM

Submitted October 3, 2006, and accepted for publication May 7, 2007.

Address reprint requests to Prof. Massimo Coletta, Dept. of Experimental Medicine and Biochemical Sciences, University of Roma Tor Vergata, Via Montpellier 1, I-00133 Rome, Italy. Tel.: 39-06-72596365; Fax: 39-06-72596353; E-mail: coletta@seneca.uniroma2.it.

Editor: Feng Gai.

0006-3495/07/09/2135/08 $2.00

doi: 10.1529/biophysj.106.098764

for RR and electronic absorption spectroscopy, and 10 μM for the kinetic measurements.

Absorption spectroscopy was been carried out at 20°C employing a Jasco V-53 spectrophotometer or a double-beam Cary 5 spectrophotometer (Varian, Palo Alto, CA). The scan speed was 120 nm/min with 2-nm resolution.

Resonance Raman (RR) spectra were measured with 413.1 nm excitation (Kr^+ laser, Coherent, Innova 300 C, Santa Clara, CA). The spectra were recorded using samples in slowly rotating NMR tubes (backscattering), employing either a double monochromator (Jobin-Yvon HG2S, Villeneuve d'Ascq, France), equipped with a cooled photomultiplier (RCA C31034A, Burle Industries GmbH, Baesweiler, Germany) and photon-counting electronics or else a triple spectrometer (consisting of two Acton Research SpectraPro2300i and a SpectraPro 2500i in the final stage with a 3600 grooves/mm grating) (Acton, MA) working on a subtractive mode and equipped with a liquid nitrogen–cooled CCD detector (Roper Scientific Princeton Instruments, Trenton, NJ).

The spectral resolution was 5 cm^{-1}. The RR spectra were calibrated to an accuracy of ± 1 cm^{-1} for intense isolated bands, with indene as standard for the high-frequency region and with both indene and CCl_4 for the low-frequency region.

Rapid-mixing stopped-flow experiments have been carried out at 20°C employing an SX.18MV apparatus with diode array (Applied Photophysics, UK). The spectra are collected with a time resolution of 1.5 ms. In addition, measurements have also been carried at a single wavelength (which makes it impossible to improve both the time and the signal/noise resolution), obtaining the same results as with the diode array. The sodium azide concentration dependence at pH 7.0 has been undertaken mixing the ferric form of the hemoprotein in 100 mM phosphate with the same buffer containing various amounts of sodium azide over the investigated concentration range.

RESULTS

Spectroscopy of ferric horse heart Mb and mini Mb

Fig. 1 *A* shows the absorption spectra of ferric HHMb and of mini Mb, together with the spectrum of the ferric HHMb/imidazole complex. The mini Mb spectrum differs from the mother protein, showing a Soret band maximum at 411 nm (409 nm for HHMb), a red-shifted visible region with a peak at 533 nm, and a shoulder at 567 nm (at 504 nm with a shoulder at 535 nm for HHMb). Moreover, the charge-transfer band (CT1), observed at 634 nm in HHMb, decreases in intensity in mini Mb, giving rise to a shoulder at 636 nm. All these features, including the similarity with the spectrum of the HHMb/imidazole complex (bands at 414, 533, and 567 nm), clearly indicate a difference in the heme iron coordination between HHMb and mini Mb, suggesting the presence of a hexacoordinated low-spin (6c LS) form in mini Mb. This is confirmed by the RR spectra (Fig. 1 *B*). The high-frequency RR spectrum of ferric HHMb shows the features of an aquo six-coordinated high-spin (6cHS) heme [1482(ν_3), 1513 (ν_{38}), 1544 (ν_{11}), 1563 (ν_2), 1580 (ν_{37}) cm^{-1}]. Moreover, the intense band at 1621 cm^{-1} is caused by the two ν(C=C) stretching modes (14). The spectral changes observed for mini Mb indicate the formation of a 6cLS heme [1505 (ν_3), 1550 (ν_{38}), 1562 (ν_{11}), 1580 (ν_2), 1601 (ν_{37}), 1641 (ν_{10}) cm^{-1}] coexisting with a minor 6cHS form (as judged by the bands at 1480 (ν_3) and 1563 (ν_2) cm^{-1}). Moreover, in the vinyl stretching region, two

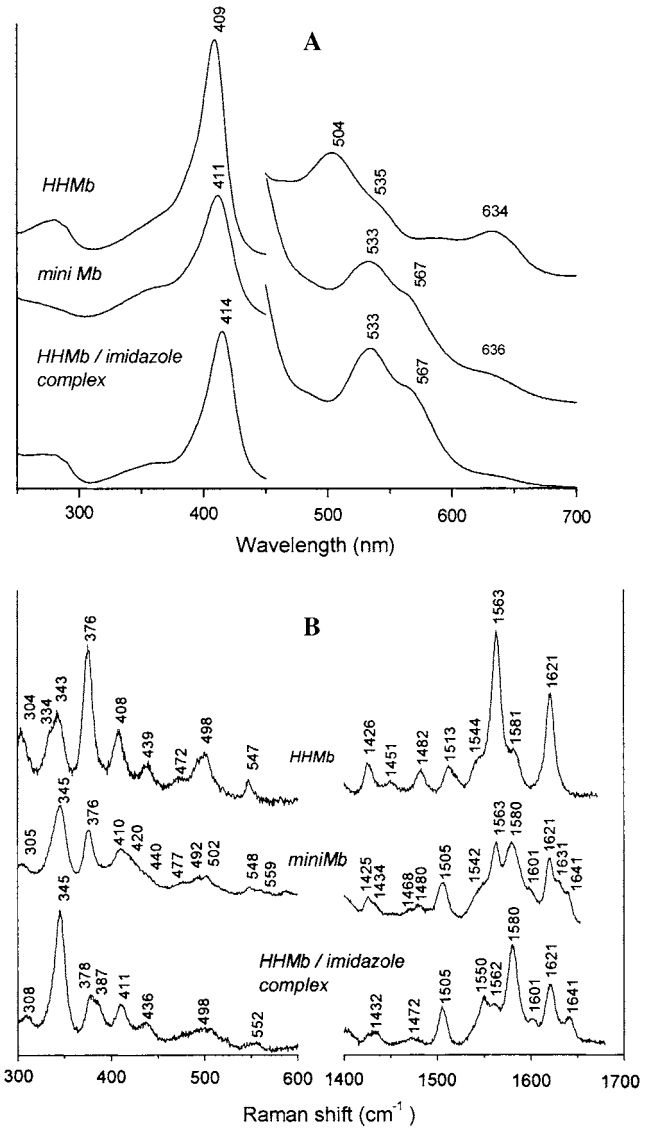

FIGURE 1 (*A*) Electronic absorption spectra of ferric horse heart Mb (HHMb), mini Mb at pH 7.0 in 100 mM phosphate, and Mb/imidazole complex ([Imidazole] = 0.18 M) in 0.1 M Tris, pH 8.4. The 450–700-nm region has been expanded by a factor of eight. (*B*) Corresponding RR spectra in the low- and high-frequency regions using 413.1-nm excitation wavelength. Experimental conditions: HHMb, 1 s/0.5 cm^{-1} and 2 s/0.5 cm^{-1} accumulation time for the high- and low-frequency regions, respectively; 15-mW laser power at the sample; mini Mb, 900 s accumulation time, 12-mW laser power at the sample; Mb-Imidazole, 2 s/0.5 cm^{-1} accumulation time and 20-mW laser power at the sample. The relative intensities of the RR bands are normalized on the ν_4 band (not shown). The low-frequency region has been expanded by 40%.

bands at 1621 and 1632 cm^{-1} are observed that are assigned to two ν(C=C) stretching modes. Accordingly, in the low-frequency region, the vinyl bending modes, assigned in Mb to the band at 408 cm^{-1}, split in mini Mb into two bands at 410 and 420 cm^{-1}, reflecting the variations of the vinyl stretching modes observed in the high-frequency region. The RR spectra of mini Mb differ from those displayed by

HHMb bound to imidazole mainly for the relative intensity of some bands and for the frequency of the ν(C=C) stretching modes, which in the HHMb/imidazole complex show the same frequency as in HHMb (Fig. 1 *B*). However, on addition of a saturating amount of imidazole (i.e., 50 mM, see Fig. 2), the electronic absorption spectra of the imidazole complexes with HHMb and mini Mb are very similar.

Kinetics of azide binding

Kinetics of sodium azide binding has been followed employing a diode array (Fig. 3, *A* and *B*), and the analysis has been undertaken at several wavelengths (either obtaining the progress curves from the spectral changes recorded by the diode array (see Fig. 3 *C*) or else by single-wavelength measurements). In both cases, we have obtained similar results, and the presence of the isosbestic point at 416 nm allows us to rule out the formation of functional intermediates over the time range of the observation. The investigation has been carried out at several sodium azide concentrations, ranging between 0.25 mM and 1 M. The concentration dependence of the observed rate constants is reported in Fig. 4. At pH 7.0 the binding of azide to the native HHMb displays only a single exponential (see Fig. 3 *C*). Under the same experimental conditions the ferric mini Mb displays a biphasic behavior with a fast phase corresponding to ~20% of the total amplitude of the absorption change observed at all wavelengths (Fig. 3 *C*). This behavior suggests that those molecules of mini Mb that are 6cHS (~20%) react rapidly with azide, whereas the remaining 6cLS molecules (~80%) react slowly because the endogenous ligand must be replaced by exogenous azide.

From the qualitative point of view, it appears immediately evident that the fast phase of mini Mb is significantly faster

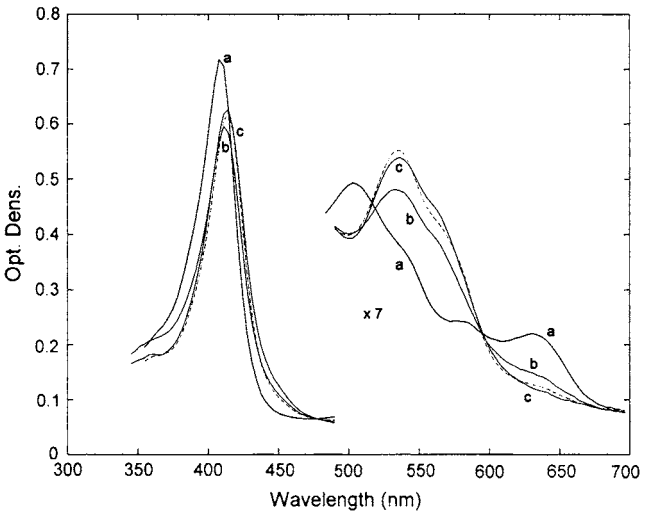

FIGURE 2 Absorption spectra in the Soret and visible regions of ferric HHMb and mini Mb on addition of 50 mM imidazole. (*a*) HHMb; (*dashed*), HHMb/imidazole; (*b*) mini Mb; and (*c*) mini Mb/imidazole. The visible region has been expanded sevenfold. For further details, see text.

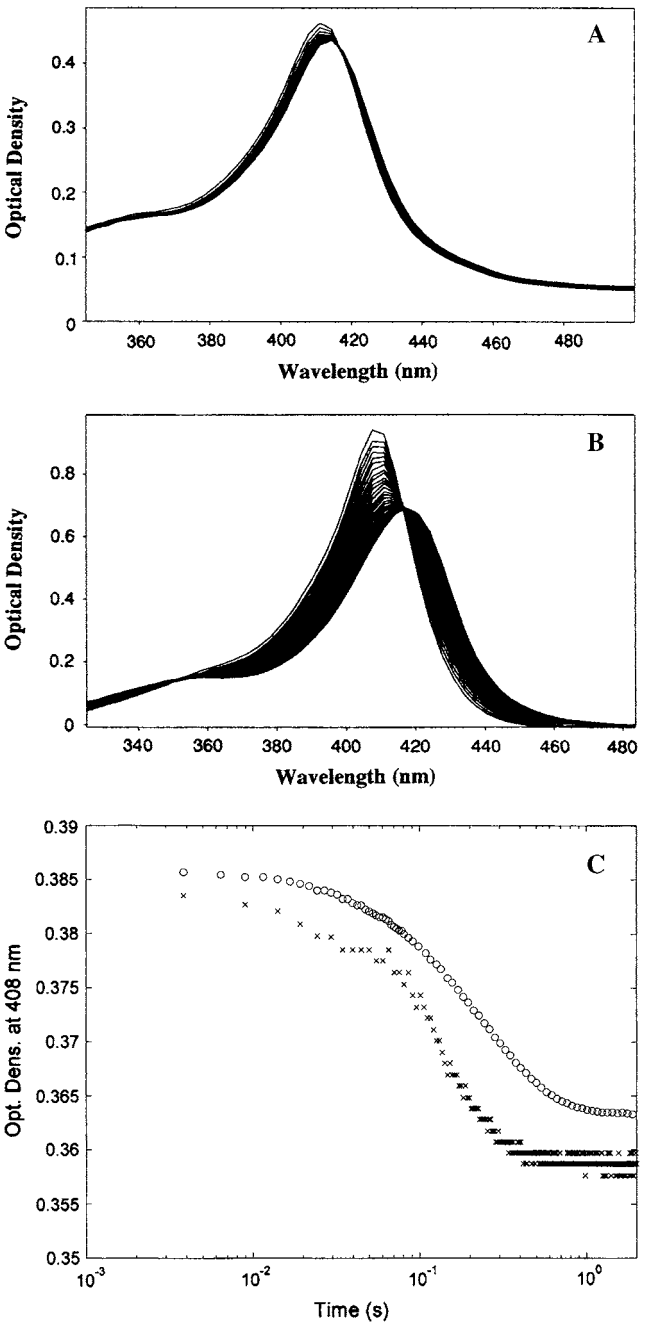

FIGURE 3 Kinetics of azide binding to HHMb and mini Mb. (*A*) Temporal evolution of absorption spectra over the first 0.3 s during the reaction of ferric mini Mb with 5 mM sodium azide at 20°C. (*B*) Temporal evolution of absorption spectra over the first 0.3 s during the reaction of ferric HHMb with 5 mM sodium azide at 20°C. (*C*) Progress curves of absorption changes at 408 nm of the reaction of ferric mini Mb (×) and of HHMb (○) with 5 mM sodium azide at pH 7.0 and 20°C. Optical changes of individual progress curves have been modified for a better comparison between them. For further details, see text.

than that of native HHMb. On the other hand, the rate constant of native HHMb resembles the slow phase displayed by mini Mb (Fig. 4). Furthermore, as previously observed for human hemoglobin and SWMb (5), the rate

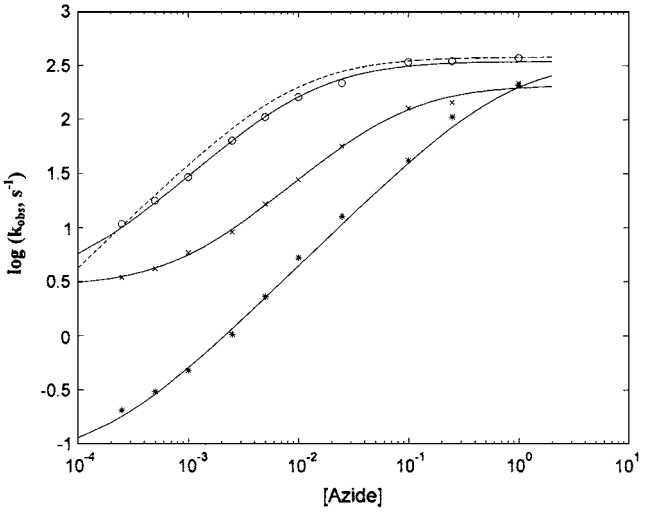

FIGURE 4 Azide concentration dependence of the observed binding rate constants. Sodium azide concentration dependence of the association rate constants at 20°C for the fast phase of mini Mb (*open circles*), slow phase of mini Mb (×), horse heart Mb (*asterisks*) and sperm whale Mb (*dashed curve*). Continuous lines have been obtained by nonlinear least-squares fitting of data according to Eq. 1 (for the fast phase of mini Mb and horse heart Mb) or Eq. 2 (for the slow phase of mini Mb) employing parameters reported in Table 1. The dashed curve has been obtained employing parameters published previously (15) and reported in Table 1 for comparison. For further details, see text.

constant levels off at high ligand concentrations, which is indicative of a rate-limiting step. This is possibly referable to the dissociation of the axial ligand coordinated to Fe(III) (e.g., H_2O for 6cHS species) before azide binding occurs.

A quantitative analysis of the concentration dependence of the observed rate constants for azide binding to HHMb (where a single species is observed, see Fig. 3 *B*) should be based on a mechanism, as follows:

$$\text{P-L} \underset{k_L}{\overset{k'_L}{\leftrightarrows}} \text{P} + \text{L} + \text{N}_3^- \underset{k'_{N3}}{\overset{k_{N3}}{\leftrightarrows}} \text{P-N}_3^-$$

SCHEME 1

where k_L and k'_L are the dissociation rate constant and the association rate constant, respectively, for the P-L complex (where L may be H_2O for the 6cHS species of intact HHMb) and k_{N3} and k'_{N3} are the dissociation rate constant and the association rate constant, respectively, for the azide binding. According to Scheme 1, the concentration dependence of the observed rate constant (i.e., k_{obs}) for azide binding is described by the following equation (5):

$$k_{obs} = \frac{k_L[N_3^-]}{\left(\frac{1}{\tau} + [N_3^-]\right)} + \frac{k_{N3}}{\tau\left(\frac{1}{\tau} + [N_3^-]\right)}, \qquad (1)$$

where *k*s have the same meaning as in Scheme 1, $[N_3^-]$ is the concentration of sodium azide, and τ ($= k'_{N3}/k'_L$) is the ratio between the association rate constants for sodium azide and those for L, indicating the competition between the two events when we have free P, which is the only species reacting with sodium azide (see Scheme 1). Parameters from Scheme 1 for HHMb have been obtained by a nonlinear least-squares fitting of experimental data according to Eq. 2 (see Table 1), and they correspond to the continuous line in Fig. 4.

The biphasic azide binding kinetics observed for mini Mb (see Fig. 3 *C*) results from the existence of two species, a prevalent 6cLS form (possibly caused by the axial coordination of an endogenous ligand, such as a distal residue) and a minor 6cHS form (likely referring to a H_2O molecule weakly bound to Fe(III)). This observation is in line with the static spectroscopic data (see Fig. 1), and the reaction scheme turns out to be somewhat more complex, as follows

$$\begin{array}{ccccc} & k'_L & & k_H & \\ \text{P-L} & \rightleftharpoons & \text{L} + \text{P} + \text{H} & \rightleftharpoons & \text{P-H} \\ & k_L & + & k'_H & \\ & & N_3^- & & \\ & & \downarrow\uparrow & & \\ & & k'_{N3} \quad k_{N3} & & \\ & & \downarrow & & \\ & & \text{P-N}_3^- & & \end{array}$$

SCHEME 2

where P-L refers to the 6cHS species (as in Scheme 1) and P-H refers to the 6cLS form (which is present in the mini Mb but not in HHMb). Therefore, parameters have the same meaning as in Scheme 1, and k'_H and k_H are the association and dissociation rate constant, respectively, for the interaction of the endogenous ligand with Fe(III). As a consequence, the azide concentration dependence of the rate constant for the fast phase of mini Mb has been analyzed employing Eq. 1, and the azide concentration dependence of the rate constant for the slow phase of mini Mb has been analyzed according to the following equation:

$$k_{obs} = \frac{k_H[N_3^-]}{\left([N_3^-] + \frac{1}{\delta}\right)} + \frac{k_{N3}}{\delta\left([N_3^-] + \frac{1}{\delta}\right)}, \qquad (2)$$

where k_{obs}, k_{N3}, and $[N_3^-]$ have the same meaning as in Eq. 1, whereas k_H is the dissociation rate constant for the ligand of the 6cLS species, and δ ($= k'_{N3}/k'_H$) is the ratio between the association rate constants for sodium azide and for H, indicating the competition between the two events when we have free P, which is the only species reacting with sodium azide (see Schemes 1and 2). Obviously, k'_{N3} and k_{N3} must be the same in Eq. 1 and in Eq. 2 for mini Mb; thus, this constraint has been imposed on the nonlinear least-squares global fitting of kinetic data from mini Mb according to Eqs. 1 and 2, and the parameters are reported

TABLE 1 Kinetic parameters from Schemes 1 and 2 for sodium azide binding to HHMb, mini Mb, and sperm whale Mb (SWMb) at pH 7.0 and 20°C

	SWMb	HHMb	Mini Mb
k_L (s^{-1})	380 ± 42	360 ± 53	348 ± 51
k_{N3} (s^{-1})	0.068 ± 0.008	0.069 ± 0.008	2.81 ± 0.32
τ	110 ± 15	1.22 ± 0.13	84.8 ± 9.2
k_H (s^{-1})	—	—	210 ± 33
δ	—	—	13.7 ± 1.8

in Table 1. It must be pointed out that at very high sodium azide concentrations (i.e., $[N_3^-] > 25$ mM), kinetics of ligand binding to mini Mb have also been followed at single wavelengths to optimize the time resolution of the fast kinetic events.

DISCUSSION

The reactivity of ferric Mb toward anionic ligands such as azide, cyanide, and fluoride has been previously investigated, mainly focusing on SWMb, on its site-directed mutants (4,5), and on the molluscan Mb (1). In particular, the reactivity of SWMb toward azide seems governed mainly by the distal His^{64}, Leu^{29}, Arg^{45}, Phe^{46}, Thr^{67}, and Val^{68} (see Fig. 5), which either 1), directly regulate the ligand access to the heme pocket (e.g., His^{64}, Leu^{29}, and Val^{68}) or 2), affect the position of the distal histidine (e.g., Phe^{46}), or else 3), modulate the hydrogen bonding of the distal side (e.g., Arg^{45}). In addition, Thr^{67} has been proposed to play a role in forming a polar channel, decreasing the energy barrier for ligand entry into the heme pocket through the interaction of its hydroxyl group with H_2O molecules solvating azide (4). An additional important factor is the presence of the H_2O molecule axially coordinated to the Fe(III), which is unveiled by the leveling off of the observed binding rate constant at high ligand concentrations (5). Therefore, the amino acids may play a role in the binding kinetics not only by modulating the access of the exogenous ligand into the heme pocket but also by affecting the relaxation time of the coordinated H_2O with the bulk solution.

HHMb displays a much smaller tendency to exchange the coordinated H_2O than SWMb, as observed by NMR

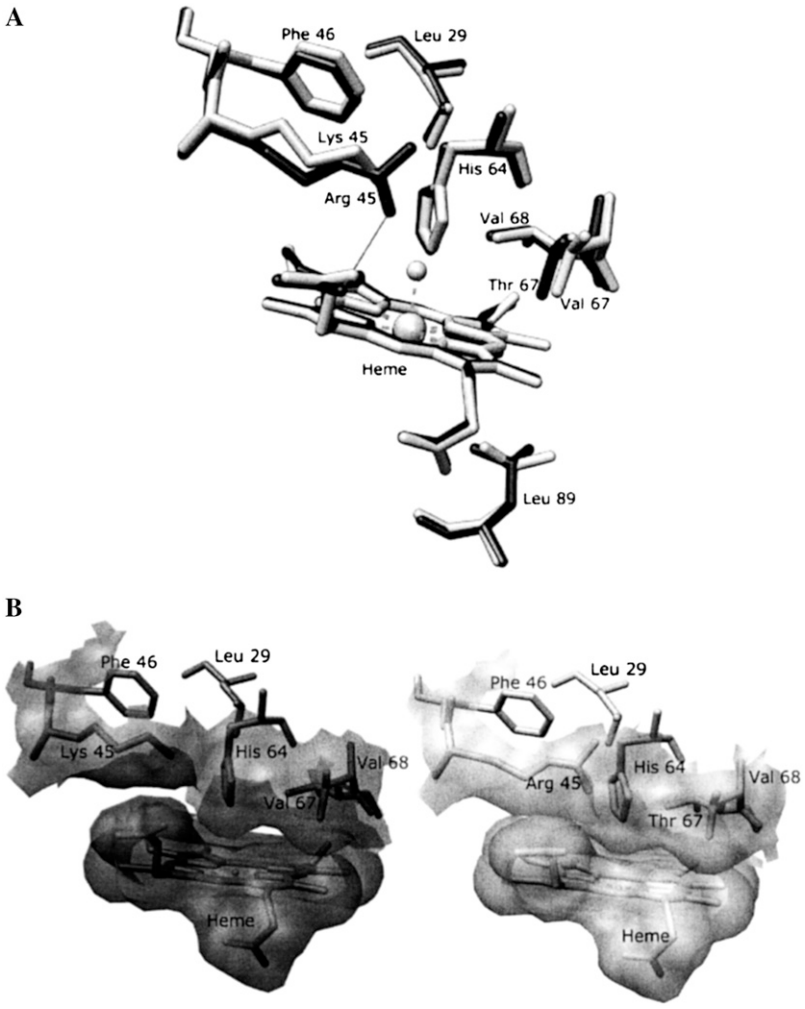

FIGURE 5 Structural comparison of the heme pocket of sperm whale Mb and of horse heart Mb. (*A*) Overlapping of residues Leu^{29}, Lys $(Arg)^{45}$, Phe^{46}, His^{64}, Val $(Thr)^{67}$, Val^{68}, and Leu^{89} in the proximity of the heme for sperm whale Mb (*dark sticks*) and horse heart Mb (*light sticks*). The H bond of Arg^{45} with heme-6-propionate is shown. (*B*) Comparison of the solvent-accessible surface for the side chains of residues Lys $(Arg)^{45}$, His^{64}, Val $(Thr)^{67}$, and Val^{68} of the Fe(III) forms of sperm whale Mb (*right*) and horse heart Mb (*left*) distal pocket (SWMb, Protein Data Bank code 1VXG; HHMb, Protein Data Bank code 1WLA). Molecular graphics images were produced using the UCSF Chimera package (23). For further details see text.

relaxometry (15). No obvious structural explanation has been found for this behavior because the only different amino acids in the heme pocket of the two proteins are Lys^{45} and Val^{67} in HHMb and Arg^{45} and Thr^{67} in SWMb (see Fig. 5). On the other hand, a comparison of the structural arrangement of the two Mbs shows some slight differences. The Arg^{45} residue of SWMb can control the rotation of His^{64} via the H bonds to the Asp^{60} residue and the heme-6-propionate groups (16). Conversely, the Lys^{45} of HHMb is unable to form these H bonds, forming instead a salt bridge with the heme-6-propionate group (12). Consistently, the ^1H NMR shift of the His^{64} $N_\delta H$ proton is markedly different in the two Mbs (17,18), suggesting a different orientation of the His^{64} residue, which is considered as a sort of gate for ligand entry in ferric Mbs (4). In addition, a more marked steric hindrance from E7–E11 residues has been reported in HHMb, likely related to the slightly different position of Phe^{46} and to the substitution of Thr^{67} by Val in HHMb (12) (see Fig. 5 *B*). Finally, the structural arrangement of the distal residues may be also influenced by the conformation of Leu^{29}, which seems different in the two myoglobins (12) (see Fig. 5 *B*). In conclusion, an alteration of the ligand dynamics, as reported in this work, may be expected.

An extended analysis of the azide binding to HHMb provides evidence that the observed rate constant is much slower for HHMb than for SWMb, at least for $[N_3^-] < 0.1$ M (Fig. 4). This effect in HHMb can be attributed only to the very low value of the τ parameter ($= k'_{N3}/k'_L$), which represents the competition between azide and H_2O for binding the Fe(III) because the two proteins show similar dissociation rate constants for azide (i.e., k_{N3}) and for H_2O (i.e., k_L, see Table 1). Altogether, these observations can be reconciled with those obtained by NMR relaxometry (15) only by inferring that the lesser extent of exchange for the coordinated H_2O with the bulk solvent, displayed by HHMb, is caused by a very fast k'_L (see Scheme 1), which indeed may greatly contribute to decreasing the observed parameter τ value (see Table 1).

On the basis of this analysis, we propose that the coordinated H_2O in HHMb dissociates as fast as in SWMb, but it reassociates much faster than in SWMb. This results in a net marked increase of the binding strength of the H_2O molecule to Fe(III) in HHMb, which certainly may account for the NMR relaxometry observations (15). This fast reassociation should be a consequence of the much more constrained volume of the distal pocket. An alternative explanation is that the faster k'_L in HHMb is a consequence of the different conformation of the proximal residue Leu^{89}, whose side chain is rotated by $\sim 120°$ around its χ_2 torsional angle in HHMb with respect to SWMb (12) (see Fig. 5 *A*). In fact, the different conformation likely affects the steric hindrance for the ligand-linked movement of the proximal side of the heme pocket. We cannot rule out also some influence from the distal side polarity because the polar channel is altered by the replacement of Thr^{67} by Val in HHMb. This possibly either speeds up the rebinding of H_2O to the heme and/or slows down the exit of H_2O molecule and the entry of azide (see below).

In the case of mini Mb, the spectroscopic observations of the presence of a predominant 6cLS form coexisting with a minor 6cHS species (see Fig. 1) account for the biphasic reaction with azide (see Fig. 3 *C*). The azide concentration dependence of the observed rate constant shows peculiar features. The fast phase (associated with the 6cHS form) is characterized by rates much faster than those observed for HHMb (with a behavior similar to that of SWMb, see Fig. 4), whereas the slow phase (associated with the 6cLS form) appears more similar to that observed for the whole HHMb (see Fig. 4). The data reported in Table 1 underline that 1), mini Mb and HHMb display closely similar values for k_L; 2), the value of the τ parameter for mini Mb is more than 10 times higher than that for HHMb; and 3), mini Mb shows a 40-fold enhanced azide dissociation rate constant k_{N3} with respect to HHMb and SWMb. The first point clearly indicates that in mini Mb the removal of the entire A helix and part of the B and H helices (11) does not significantly alter the H_2O dissociation rate, thus implying an irrelevant role of these portions of the molecule in modulating the H_2O exchange with the bulk solvent. On the other hand, the marked increase of the τ parameter in mini Mb (see Table 1) might be related to either a decrease of k'_L and/or an increase of k'_{N3} in mini Mb as compared to HHMb. The τ increase should be a consequence of the alteration after the removal of residues such as Leu^{29} that have been proposed to play an important role in shaping the ligand pathway toward the heme pocket (4). In SWMb, the replacement of Leu^{29} by Ala brings about an almost 20-fold enhancement for the apparent association rate constant for azide (4), a parameter that corresponds to our $k_L \cdot k'_{N3}/(k'_L + k'_{N3})$ (see Eq. 1); therefore, the higher τ parameter can certainly find a reasonable structural basis in an increased k'_{N3}, related to the absence of the Leu^{29} residue. Therefore, the similarity between the apparent azide binding rate constant for SWMb and the fast phase of mini Mb is caused by a much faster k'_{N3} for mini Mb, which compensates for the much slower k'_L in SWMb, resulting in an incidentally similar τ parameter for the two proteins (see Table 1). Certainly, the absence of Leu^{29} also plays an important role in determining point 3. In fact, its substitution by Ala in SWMb induces a 100-fold increase of the apparent dissociation rate constant for azide (4), which corresponds to our $k_{N3} \cdot k'_L/(k'_L + k'_{N3})$ (see Eq. 1). Moreover, structural and spectroscopic studies on the azide complexes of wild-type and site-directed mutants of HHMb showed a displacement of Leu^{29} on azide binding (19), confirming the relevant role of this residue in determining the energetics of the interaction between HHMb and sodium azide.

The shorter polypeptide chain is certainly responsible for the 6cLS heme in mini Mb. The 6cLS form should be a result of the axial ligation of an endogenous ligand to the heme Fe(III). This interaction is impaired in HHMb, where helices A, B, and H are intact. Consistently, the dissociation rate

constant for the endogenous ligand k_H is much slower than k_L (Table 1), and the lower value of the parameter δ ($= k'_{N3}/k'_H$, see Scheme 2) with respect to the parameter τ ($= k'_{N3}/k'_L$, see Scheme 2) clearly indicates that $k'_H > k'_L$. Therefore, the affinity of the endogenous ligand ($= k'_H/k_H$) for the Fe(III) is ~9-fold higher than that of H_2O ($= k'_L/k_L$), accounting for the large predominance of the 6cLS form over the 6cHS in mini Mb (see Fig. 1). The azide binding behavior of the 6cLS species of mini Mb turns out to be similar to that of HHMb simply because of the combination of a slower dissociation rate for the endogenous ligand k_H and a better competition of this ligand in mini Mb with respect to the exogenous ligand L (i.e., $\delta > \tau$, see Table 1). Clearly, the spectroscopic data for mini Mb indicate that the complete removal of the A helix, associated with the partial removal of the B and H helices, makes the E helix more flexible, thus allowing a distal residue to approach and bind the ferric atom. The nature of this endogenous ligand is suggested to be the distal His on the basis of the close similarity between the absorption and RR spectra of the 6cLS species of the ferric and the imidazole-bound forms (Figs. 1 and 2).

The presence of two vinyl bands in the RR spectra of mini Mb compared to the single band observed in HHMb (see Fig. 1) can be related to the reduced steric hindrance of one of the two vinyls caused by the conformational change, which induces the binding of the distal His. In fact, a direct relationship between the ν(C=C) stretching frequency and the orientation of the vinyl groups, as induced by specific protein interactions, has recently been found in heme-containing peroxidases and in Mb (20). When the protein matrix exerts no constraints on the vinyl groups, they take the torsional conformation usually found in model compounds in solution (21), and two ν(C=C) stretching modes should be observed in the RR spectrum.

The lack of important H bonds (in particular the salt bridge Glu^{18}–Lys^{77}, connecting helix A and E in HHMb) could be the reason for the increased flexibility of helix E and likely of the whole mini Mb. A structural change leading to distal His coordination has been observed to occur also on surfactant treatment of HHMb, and it has been interpreted as a consequence of the rupture of key salt bridges by the surfactant molecules (22). This increased flexibility associated with the decreased steric hindrance by the protein matrix (see above) and the absence of a significant portion of the distal barrier (as a result of the partial lack of the helix B) would give support to the idea that the increased τ parameter in mini Mb is related to a marked enhancement of the bimolecular rate constant for azide binding k'_{N3} rather than to an increase of k'_L, which is instead responsible for the higher tendency of HHMb to bind H_2O (see above).

The authors express their gratitude to Prof. P. Ascenzi for several fruitful discussions and to Dr. B. Howes for critically reading the manuscript.

A financial contribution from the Italian Ministery of Education, University and Research (MIUR FIRB RBNE03PX83 to M.C.), is gratefully acknowledged.

REFERENCES

1. Giacometti, G. M., P. Ascenzi, M. Bolognesi, and M. Brunori. 1981. Reactivity of ferric *Aplysia* myoglobin towards anionic ligands in the acidic region. Proposal for a structural model. *J. Mol. Biol.* 146:363–374.
2. Smerdon, S. J., G. G. Dodson, A. J. Wilkinson, Q. H. Gibson, R. S. Blackmore, T. E. Carter, and J. S. Olson. 1991. Distal pocket polarity in ligand binding to myoglobin: structural and functional characterization of a threonine68(E11) mutant. *Biochemistry.* 30:6252–6260.
3. Cutruzzola, F., C. Travaglini Allocatelli, P. Ascenzi, M. Bolognesi, S. G. Sligar, and M. Brunori. 1991. Control and recognition of anionic ligands in myoglobin. *FEBS Lett.* 282:281–284.
4. Brancaccio, A., F. Cutruzzola, C. Travaglini Allocatelli, M. Brunori, S. J. Smerdon, A. J. Wilkinson, Y. Dou, D. Keenan, M. Ikeda-Saito, R. E. Brantley Jr., and J. S. Olson. 1994. Structural factors governing azide and cyanide binding to mammalian metmyoglobins. *J. Biol. Chem.* 269:13843–13853.
5. Coletta, M., M. Angeletti, G. De Sanctis, L. Cerroni, B. Giardina, G. Amiconi, and P. Ascenzi. 1996. Kinetic evidence for the existence of a rate-limiting step in the reaction of ferric hemoproteins with anionic ligands. *Eur. J. Biochem.* 235:49–53.
6. Winkler, W. C., G. Gonzalez, J. B. Wittenberg, R. Hille, N. Dakappagari, A. Jacob, L. A. Gonzalez, and M. A. Gilles-Gonzalez. 1996. Nonsteric factors dominate binding of nitric oxide, azide, imidazole, cyanide, and fluoride to the rhizobial heme-based oxygen sensor FixL. *Chem. Biol.* 3:841–850.
7. Milani, M., Y. Ouellet, H. Ouellet, A. Boffi, G. Antonini, A. Bocedi, M. Mattu, M. Bolognesi, and P. Ascenzi. 2004. Cyanide binding to truncated hemoglobins: a crystallographic and kinetic study. *Biochemistry.* 43:5213–5221.
8. Herold, S., A. Fago, R. E. Weber, S. Dewilde, and L. Moens. 2004. Reactivity studies of the Fe(III) and Fe(II)NO forms of human neuroglobin reveal a potential role against oxidative stress. *J. Biol. Chem.* 279:22841–22847.
9. Travaglini Allocatelli, C., F. Cutruzzola, A. Brancaccio, M. Brunori, J. Qin, and G. N. La Mar. 1993. Structural and functional characterization of sperm whale myoglobin mutants: role of arginine (E10) in ligand stabilization. *Biochemistry.* 32:6041–6049.
10. Bolognesi, M., S. Onesti, G. Gatti, A. Coda, P. Ascenzi, and M. Brunori. 1989. *Aplysia limacina* myoglobin. Crystallographic analysis at 1.6 A resolution. *J. Mol. Biol.* 205:529–544.
11. De Sanctis, G., G. Falcioni, B. Giardina, F. Ascoli, and M. Brunori. 1986. Mini-myoglobin: preparation and reaction with oxygen and carbon monoxide. *J. Mol. Biol.* 188:73–76.
12. Evans, S. V., and G. D. Brayer. 1990. High-resolution study of the three-dimensional structure of horse heart metmyoglobin. *J. Mol. Biol.* 213:885–897.
13. Antonini, E., and M. Brunori. 1971. Hemoglogin and Myoglobin in Their Reactions with Ligands. North-Holland, Amsterdam.
14. Choi, S., T. G. Spiro, K. C. Langry, K. M. Smith, D. L. Budd, and G. N. La Mar. 1982. Structural correlations and vinyl influences in resonance Raman spectra of protoheme complexes and proteins. *J. Am. Chem. Soc.* 104:4345–4351.
15. Aime, S., P. Ascenzi, M. Fasano, and S. Paletti. 1993. NMR relaxometric studies of water accessibility to haem cavity in horse heart and sperm whale myoglobin. *Magnet. Reson. Chem.* 31:585–589.
16. Takano, T. 1977. Structure of myoglobin refined at 2.0 Å resolution. I. Crystallographic refinement of metmyoglobin from sperm whale. *J. Mol. Biol.* 110:537–568.
17. Morishima, I., and M. Hara. 1983. High-pressure nuclear magnetic resonance studies of hemoproteins. Pressure-induced structural changes in the heme environments of ferric low-spin metmyoglobin complexes. *Biochemistry.* 22:4102–4107.
18. Kitahara, R., M. Kato, and Y. Taniguchi. 2003. High-pressure ^{1}H NMR study of pressure-induced structural changes in the heme environments of metcyanomyoglobins. *Protein Sci.* 12:207–217.

19. Maurus, R., R. Bogumil, N. T. Nguyen, A. G. Mauk, and G. Brayer. 1998. Structural and spectroscopic studies of azide complexes of horse heart myoglobin and the His-64 → Thr variant. *Biochem. J.* 332:67–74.

20. Marzocchi, M. P., and G. Smulevich. 2003. Relationship between heme vinyl conformation and the protein matrix in peroxidases. *J. Raman Spectrosc.* 34:725–736.

21. Kalsbeck, W. A., A. Ghosh, R. K. Pandey, K. M. Smith, and D. F. Bocian. 1995. Determinants of the vinyl stretching frequency in protoporphyrins. Implications for cofactor-protein interactions in heme proteins. *J. Am. Chem. Soc.* 117:10959–10968.

22. Tofani, L., A. Feis, R. E. Snoke, D. Berti, P. Baglioni, and G. Smulevich. 2004. Spectroscopic and interfacial properties of myoglobin/surfactant complexes. *Biophys. J.* 87:1186–1195.

23. Pettersen, E. F., T. D. Goddard, C. C. Huang, G. S. Couch, D. M. Greenblatt, E. C. Meng, and T. E. Ferrin. 2004. UCSF Chimera. A Visualization System for Exploratory Research and Analysis. *J. Comput. Chem.* 25:1605–1612.